PHYSICAL REVIEW B VOLUME 28, NUMBER 9 1 NOVEMBER 1983

Effect of hydrogen-isotope implantation on aluminum oxide tunnel-junction barriers

J. Igalson* and J. G. Adler
Department of Physics, University of Alberta, Edmonton, Alberta T6G 2J1, Canada
(Received 26 April 1983)

This paper compares aluminum oxide tunnel junctions prepared by standard plasma techniques with those made with the use of an ion gun. The effect of hydrogen and deuterium implantation on the barriers has been studied in detail both in terms of the inelastic electron tunneling spectra and the change in work function produced at the metal-oxide interfaces. The results indicate that there is an upper limit on the amount of hydrogen which may be present in the oxide barrier. The results further suggest that the peak in the inelastic electron tunneling spectrum at 230 meV (1850 cm^{-1}) may be due to aluminum hydride.

I. INTRODUCTION

In recent years there has been an increasing interest in inelastic electron tunneling spectroscopy (IETS).[1] An essential component in junction fabrication is the insulating barrier, which in a vast majority of cases is made of aluminum oxide. A great deal of effort has been concentrated on identifying the oxide of such typical Al-oxide—metal junctions.[2–7] A detailed understanding of the type of aluminum oxide barrier is crucial to the development of IETS since these barriers form the active surface on which chemisorbed species are studied. Previous work on these oxide barriers[2–5,7] showed the effect of OH groups and H_2O (Refs. 8—10) with them.

The present paper extends these previous studies by observing specifically the effect of implanted hydrogen and deuterium on these oxides, as well as the use of a new preparation technique using an ion gun for oxide growth. By studying the inelastic spectra, which tells us about the barrier vibrational modes and the elastic tunneling from which we obtain values of the effective work functions of the two metal electrodes in the junction environment, we obtain information on the OH groups and their distribution in the oxide. By observing annealing effects[11–13] in these implanted junctions we are able to follow changes in the charge structure of the barriers and find that there exists an equilibrium concentration of OH dipoles in oxide tunnel barriers.

II. EXPERIMENTAL

Al-oxide—Pb planar tunnel junctions were prepared in a diffusion-pumped liquid-nitrogen-trapped vacuum system which was pumped to the 40-μPa range. A large surface liquid-nitrogen trap above the junction preparation area could be activated to further reduce the pressure and thus also the amount of water vapor present during fabrication. The junctions were prepared on clean fire-polished Pyrex substrates, two junctions per substrate. Following deposition of silver contacts an aluminum base layer of ~ 200 nm was evaporated at a rate of ~ 2 nm/s. Two types of barriers were made. The first of these will be referred to as a plasma oxide and the second as a gun oxide. The plasma oxides were prepared by exposing the freshly evaporated aluminum films to a pure oxygen plasma having a pressure of 26 Pa for about 3 min. The plasma was excited by an ionizing field of ~ 70 kV/m and a current of 15 mA. The gun oxides were prepared using a saddle-field ion source.[14–16] This type of ion source allows operation at much lower pressures than the conventional plasma oxidation described above. In this type of source electrons oscillate in a saddle field between two cathodes. These electrons produce ionization by collision during their oscillations. The anode and shield configuration are arranged in such a way that many of the ions recombine with secondary electrons producing a high proportion of energetic neutrals. This is important since it avoids charging of the aluminum during oxide growth or during hydrogen or deuterium implantation. For gun oxides the ion gun was usually operated at a cathode potential of ~ -1 kV. In this configuration the ionizing plasma was produced by a saddle field of ~ 300 kV/m. Prior to oxidation using the ion gun the system was pumped below 40 μPa, while during oxidation ($\sim$8-min exposures) the overall system pressure never rose above 5 mPa. (The total pressure in the vicinity of the substrates being considerably lower since the liquid-nitrogen trap above the substrate was used during this operation.) The composition of the background vacuum was <5 vol % H_2, ~ 60—70 vol % H_2O, ~ 15 vol % N_2+CO, ~ 8 vol % CO_2, and <1 vol % Ar. The ion gun was operated with an oxygen flux of 2×10^{23} m^2/s^{-1}. During oxidation the partial pressures (measured 0.3 m away from the substrate) were $H_2<1$ vol %, $H_2O\sim 10$ vol %, N_2+CO ~ 5 vol %, $O_2\sim 75$—80 vol %, and $CO_2<5$ vol %. The same gun and a similar procedure were also used to implant hydrogen and deuterium into some of the oxides. Junction preparation was completed by a 200-nm layer of Pb deposited at a rate of ~ 1 nm/s. Implantation time for hydrogen varied from 0.5 to 1 min, while that for deuterium varied from 0.5 to 2 min. Exposures for times longer than these were found to produce high-resistance junctions which did not withstand thermal cycling. For most of the experiments implantation was carried out prior to depositing the Pb cover electrode, but in some instances implantation was carried out through the Pb overlayer. The entire junction

 ©1983 The American Physical Society

fabrication and implantation was carried out without breaking vacuum, the finished junctions were mounted and stored at 77 K within less than 5 min of fabrication. The measurements on the finished junctions were all carried out at 4.2 K. The dynamic conductance $\sigma = dI/dV$ (where I is the junction current and V the junction bias) and its derivative $d\sigma/dV = d^2I/dV^2$ were measured using a bridge system similar to that of Adler and Straus[17] with an on-line computer providing calibration.[18]

Measurements were carried out on fresh (virgin) junctions and in many instances on aged (annealed) junctions. Junctions for annealing were warmed in a vacuum to prevent condensation from destroying them. The annealing also took place in a vacuum and was performed at room temperature. Two types of annealing methods were used: Thermal annealing where the junction was aged with its four terminals in an open-circuit configuration and voltage annealing in which a 0.7-V bias was supplied between the Al and Pb films during annealing. In this later process two configurations were used: Forward polarity (FP) where the Al film was held positive and reverse polarity (RP) where the Al film was negative during the annealing process. At various times the annealing was interrupted, the junction returned to 4.2 K and σ and $d\sigma/dV$ measured over a range of ± 500 mV. These measurements not only provided the IET spectrum but enabled a determination of the work functions ϕ_1 at the Al electrode and ϕ_2 at the Pb electrode. These work functions were determined assuming a trapezoidal barrier using the procedure of Brinkman, Dynes, and Rowell.[19]

III. RESULTS AND DISCUSSION

A. Barrier preparation effects

The tunneling spectrum of a typical plasma-oxide junction is shown in curve a in Fig. 1. It is interesting to note that these junctions have a very characteristic spectrum in spite of the fact that plasma geometry, current, and voltage, as well as oxygen pressure, vary considerably from laboratory to laboratory.[3–9] The most prominent difference among such junctions is the occasional appearance of small C—H bending peaks (~130 meV) and C—H stretching peaks (~360 meV) observed when the vacuum system used in junction preparation is not scrupulously clean. This is in marked contrast with thermal oxides which often vary considerably from preparation to preparation and are prone to hydrocarbon contamination. In our evaporator the discharge ring used for the oxidizing plasma extends over most of the cross section (~0.4 m diam) of the vacuum system. Such a large extent makes cleaning difficult. With the use of a small ion gun to restrict plasma volume (~0.08 sr and gun to substrate separation of ~0.035 m) it was hoped to produce ultraclean oxides. Curve b in Fig. 1 shows a typical gun oxide. It can be seen that both types of oxide are relatively free from hydrocarbon contamination as evidenced from the absence of structure at 130 ad 360 meV. Here, however, the similarity ends; the gun oxide differs from the plasma oxide in that it has more structure in the vicinity of 80 and 230 meV, while the Al—O stretch (~115 meV) is broader and

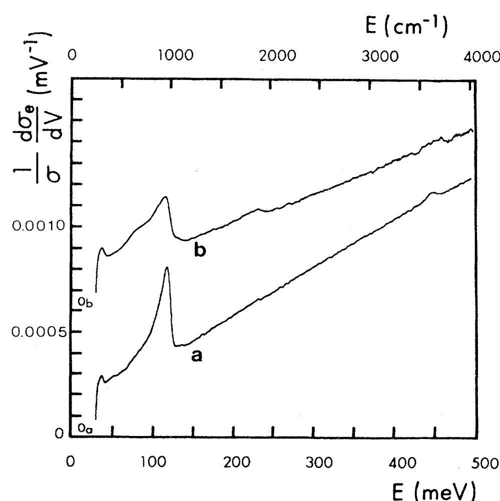

FIG. 1. IET spectra for Al-oxide—Pb junctions. Curve a represents a conventional plasma oxide, while curve b is the spectrum of a gun oxide. σ_e is the even part of the junction dynamic conductance dI/dV. The curves are offset for clarity, 0_a and 0_b represent the zero levels of the two curves, respectively.

more subdued. This 115-meV peak has been the cause of some uncertainty in the past being ascribed to an alumina hydrate mode [Al—OH bend (Refs. 2 and 3)] and in part to Al—O stretching mode,[5] the latter probably contributing most to the peak intensity. Unfortunately it is impossible to completely eliminate hydrogen from a vacuum system particularly where many stainless-steel parts are involved, hence alumina hydrate contributions to the 115-meV peak are hard to evaluate quantitatively. The conventional interpretation of the 80-meV peak is that it is due to O—H bending modes, while the structure near 230 meV has been described as a harmonic of the 115-meV peak.[2–7] It is evident that there is somewhat less than the usual surface O—H stretching mode intensity (~450 meV) present in these junctions, suggesting a relatively dry junction fabrication environment than usual.[5–7] In fact, the relative lack of such structure near 450 meV in all our junctions is probably due to the use of a liquid-nitrogen trap above the specimen during preparation. It has been shown[21,22] that when an Al surface oxidizes, place exchange occurs in such a way that some of the oxygen penetrates beneath the Al surface. It is this subsurface oxygen which along with the Al produces an outward pointing (negative to positive charge) dipole which serves to reduce the work function of Al upon oxygen adsorption. This work-function lowering is most pronounced on the low-index planes where it has been found to reduce the work function by as much as 1.1 eV.[23] The actual reduction of work function depends on the net surface polarization established between the competing subsurface O-Al and supersurface Al-O dipoles. In systems used in tunnel-junction preparation a good deal of water and hydrogen are also present and may produce O—H bonds, again with the dipole moment pointing away from the Al surface, further reducing the work function at the Al sur-

TABLE I. Results calculated from the dynamic conductance curves of our tunnel junctions.

Preparation method	ϕ_1 (eV)	ϕ_2 (eV)
Plasma oxide	1.8–2.0	4.0–4.2
Gun oxide	2.0–2.3	4.0–4.5
Gun oxide plus hydrogen	1.2–1.5	4.8–5.0
Gun oxide plus deuterium	1.2–1.3	5.0–5.5

face, ϕ_1.[24] Some possible configurations of such AlO_x surfaces have been discussed recently by Dragoset, Phillips, and Coleman.[7] Our results obtained from an analysis of the dynamic conductance of our tunnel junctions using the trapezoidal barrier of Brinkman, Dynes, and Rowell[19] are shown in Table I. These data are generally consistent with those in the literature.[7] We also note that the value of ϕ_2 for the Pb side of the junction is somewhat increased over that of pure lead ($\phi \sim 4$ eV). This increase is associated with hydroxyl groups present on the oxide surface beneath the Pb with their dipole moments pointed towards the Pb surface. We shall return to a more detailed discussion of these results after considering the effect of hydrogen implantation.

B. Hydrogen and deuterium implantation

Having commented on the essential differences between the gun and the plasma oxide we turn our attention to junctions in which hydrogen or deuterium was implanted after oxide formation. The saddle-field ion source described above was used to implant the two hydrogen isotopes. Curve b in Fig. 2 shows the effect of hydrogen implantation on the IET spectrum of a plasma-oxidized junction of the type depicted in curve a in Fig. 2. The effects of hydrogen and deuterium implantation on a gun oxide are depicted in the upper three curves of Fig. 2. There are pronounced increases in the O—H stretching mode near 450 meV and the O—D stretching mode in the vicinity of 331 meV. Similar increases are manifest in the O—H and O—D bending modes near 80 and 52 meV. These changes can readily be associated with increasing numbers of O—H and O—D bonds.[1–10] A very prominent increase in peak height near 230 meV in the hydrogen-implanted junctions and near 167 meV in the deuterated spectra is evident. As discussed, the structure observed in the vicinity of 230 meV in Al-AlO_x—Pb junctions has been associated with a harmonic of the Al—O stretching mode at 115 meV.[5] Certainly if the 115-meV structure was solely due to the harmonic of the Al—O stretching mode it would be surprising indeed if it was so much enhanced by hydrogen implantation. One possibility that could also be considered is the formation of aluminum hydride during junction fabrication since an Al—H stretching mode would be expected near 230 meV.[25] Junction fabrication is usually carried out in stainless-steel vacuum systems, and thus hydrogen background concentration may be high. We focus our attention now on the work functions shown in Table I. It is clear that the implanta-

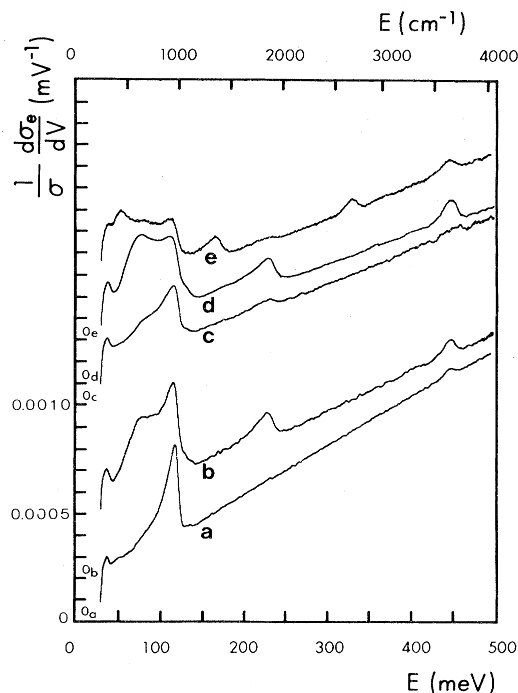

FIG. 2. IET spectrum of a clean plasma oxide (curve a) and a plasma oxide with a 1-min hydrogen implantation (curve b). IET spectrum of a clean gun oxide (curve c), a gun-oxide implanted with hydrogen for 1 min (curve d), and a gun with a 2-min deuterium implantation (curve e).

tion of the two hydrogen isotopes lowers the work function at the aluminum oxide boundary more than oxidation does. This increase in work function could be due to the presence of both highly polar O-H and slightly polar Al-H dipoles with their moments pointing away from the interface. At the Pb interface there is an increase in ϕ_2, suggesting dipoles with their moments pointing towards the metal. In this latter case the dipoles involved are probably surface O—H and surface O—D stretching modes as evidenced by the increase in the peak near 450 meV for the hydrogen and near 331 meV for the deuterium implantations.[2–5] There is also an effect due to the isotropic mass of the implant (Table I) visible at both interfaces but especially near the Pb surface where ϕ_2 rises to above 5 eV.

C. Annealing effects in hydrogen-implanted junctions

In order to better understand the structure of the oxide and to investigate the role of ion mobility, some annealing studies were carried out[11–13]; the resulting spectra appear in Fig. 3. The spectra shown are all the result of 63 h annealing at room temperature. The hydrogen-implanted virgin junction in curve a in Fig. 3 shows a significant peak due to surface O—H stretching modes near 450 meV, which diminishes upon annealing (thermal and reverse polarity) and virtually disappears when the junctions are annealed with forward polarity. The rate at which this O—H stretching peak decreases in a thermally annealed junction is illustrated in Fig. 4. The quantity $F(450)$ is a

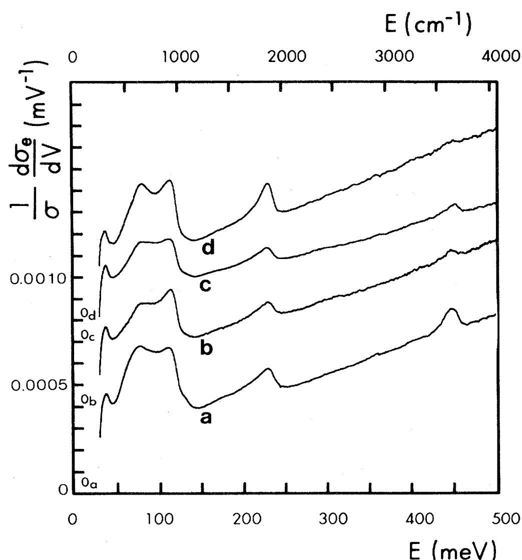

FIG. 3. Effect of annealing on a typical 1-min hydrogen-implanted gun-oxide junction. Spectrum of the fresh junction (curve *a*), thermally annealed for 63 h at room temperature (curve *b*), voltage annealed with reverse polarity (see text) for 63 h at room temperature (curve *c*), and the effect of a 63-h anneal with FP at room temperature (curve *d*). All spectra were measured at 4.2 K.

measure of the fractional change in conductance due to this O—H stretch, and is obtained from the area under the peak by

$$F(V)=\int[\sigma^{-1}(d\sigma/dV)-g(V)]dV\ ,$$

where $g(V)$ is a smooth function to the spectral curve.[8] The effect is illustrated for thermal annealing and differs immeasurably for the two isotopes. The effect of the various annealing procedures on the work functions is illustrated in Fig. 5. Let us first consider the effects in the vicinity of the lead electrode. Figure 4 clearly indicates a

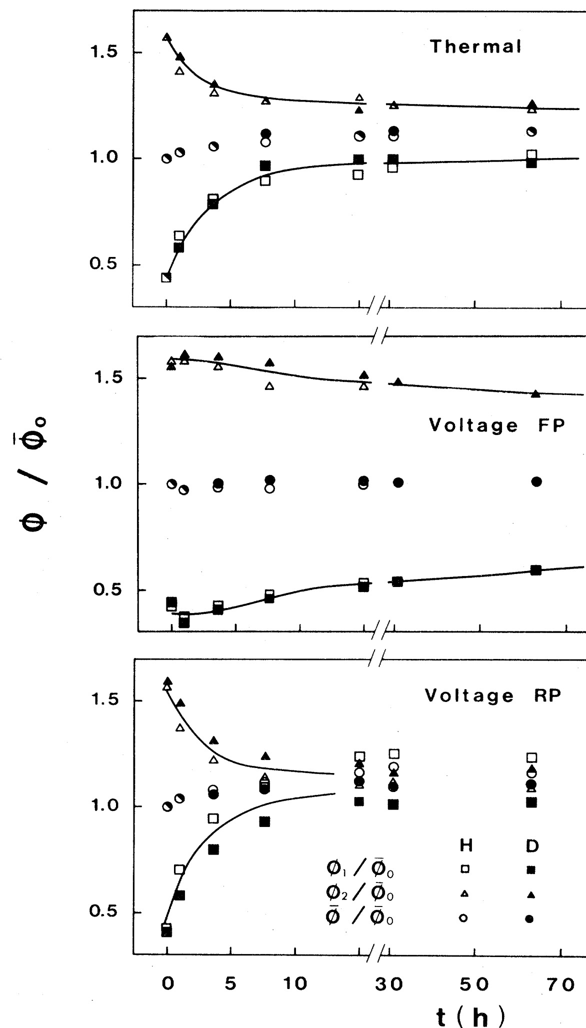

FIG. 5. Change in work functions during thermal and voltage annealing normalization to the average barrier height $\bar{\phi}_0$ of the junction prior to annealing. Results are shown for both hydrogen- and deuterium-implanted junctions.

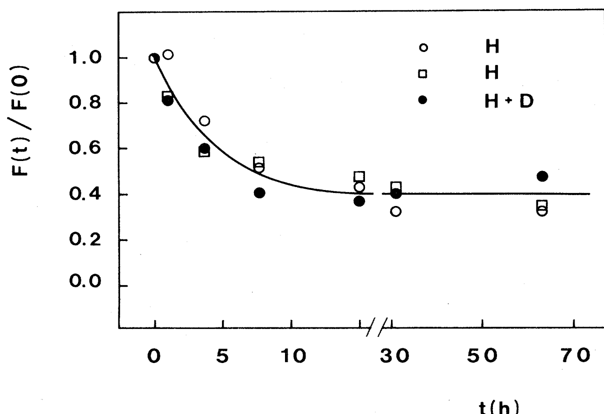

FIG. 4. Peak intensity *F*(450) of the O—H stretching mode as defined by the equation in the text normalization to its $t=0$ (peak intensity prior to annealing) *F*(0) for hydrogen- and deuterium-implanted junctions. $F(0)=2.4\times10^{-3}$.

reduction in surface O—H stretch at the oxide-Pb interface, which is in agreement with the observed decrease in ϕ_2 indicating that O-H dipoles are leaving the junction. This can be interpreted as resulting from an excess concentration of implanted hydrogen which decreases to an equilibrium value with time. This contrasts with annealing results on unimplanted junctions in which the O-H arises due to residual hydrogen and water vapor in the vacuum system.[11,12] In the unimplanted junctions[11–13] *F*(450) increases with annealing due to alignment of the O-H dipoles in the intrinsic field of the junctions with time reaching a final value near 1.25×10^{-3}, which is similar to the final value obtained for our implanted junctions. The central plot in Fig. 5 shows the effect of forward polarity on the annealing behavior of the work functions. In this case the applied field is such as to enhance the alignment of the O-H dipoles, as this alignment increases so

does the repulsion between dipoles, thus ϕ_2 initially increases with dipolar alignment (more H facing the oxide-Pb interface) then decreases as some dipoles leave the junction due to mutual repulsion. In the case of reverse polarity ϕ_2 drops quickly due to the combined effects alignment and decrease in concentration.

In the case of the Al-oxide interface we see from Fig. 5 that the Al work function increases sharply with both thermal and RP annealing suggesting that the polarization at this surface changes in such a way that there is less of a net dipole moment pointing away from the Al surface. In the case of the thermal anneal the intrinsic field of these junctions (Table I) is such as to favor alignment of dipoles with their moments away from the Al, thus suggesting that the increase in ϕ_1 that we observe is due to dipoles leaving the junction. In the case of reverse bias the effect is enhanced since this bias produces a field in a direction which helps align dipoles with their moments towards the aluminum surface. When forward polarity annealing is carried out the field helps align the dipoles with their moments away from the Al decreasing the work function; eventually, however, a few of these dipoles leave the junction resulting in a slight increase in ϕ_1.

We return now to the effect of annealing on the IET spectrum of the hydrogen-implanted junctions. It is clear from Fig. 3, especially the spectrum of the FP-annealed junction (curve *d*), that the 450-meV O—H stretching mode disappears while the 230-meV peak increases in size and sharpens up considerably, and the 115- and 80-meV peaks become somewhat better resolved. We had concluded above that the surface O-H at the oxide-Pb interface was present in excess of equilibrium and driven out of the junction by FP annealing. This also occurs but to a lesser extent in the case of the thermal and RP-annealing cases. On the other hand, the pronounced increase in the 230-meV peak eludes quick explanation.

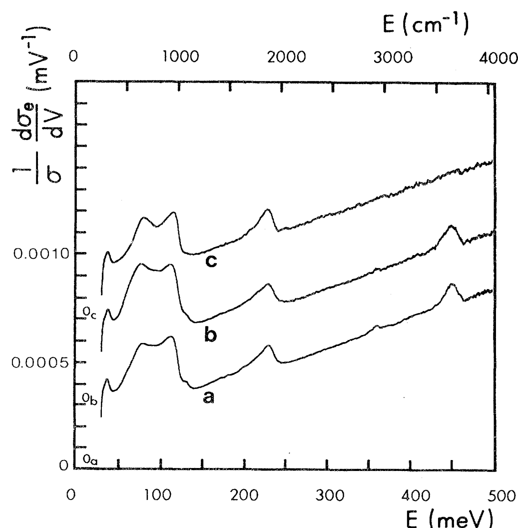

FIG. 6. Effects of various implantation processes. Spectrum (curve *a*) is for a junction implanted with hydrogen prior to formation of the oxide barrier, normal implantation on top of the oxide is shown in (curve *b*), and hydrogen implantation after evaporation of the Pb-cover electrode but prior to exposure to air (curve *c*).

D. Other observations on hydrogen implantation

We have already established that the 230-meV peak requires the presence of H or O-H during junction fabrication. The infrared and Raman spectra of aluminum hydroxides show no structure in the vicinity of this peak.[25–27] There are only scant data in the literature[28,29] on aluminum hydrides; however, it is known that the AlH^{-4} ion has a prominent peak near 222 meV. In order to try to understand the role of the implanted hydrogen a different set of implantation experiments was carried out. Pure hydrogen was implanted prior to formation of the oxide barrier, and following this, gun oxidation was carried out and the Pb cover electrode evaporated as usual; the results appear in curve *a* in Fig. 6. This result is similar to that in which the hydrogen implantation takes place after oxidation (curve *b* in 6) insofar as the 230-meV structure is concerned, but the peak near 80 meV (O—H bending) is not as pronounced. Finally junctions were implanted with hydrogen after they had been completed by evaporation of the Pb electrode but prior to exposure to air. A typical spectrum for such a junction is shown in curve *c* in 6. The pronounced 230-meV structure is again present; however, this time there is a clear absence of the O—H stretching mode at 450 meV. This latter effect is not necessarily an indication that there is no surface O-H present between the oxide and the Pb cover layer but rather that there was too little room for the O-H to stand with their moments perpendicular to the barrier and thus not contribute to the inelastic tunneling. Some of the hydrogen, however, entered the barrier providing the enhanced 80- and 230-meV peaks. Two further observations were made: When molecular hydrogen was used (no gun) there was no effect, and if junctions were exposed to air after the Pb electrode was evaporated, but prior to hydrogen implantation, then the implantation had no effect. This suggests that molcular hydrogen is too large to pass through the cracks or grain boundaries in the lead, and that exposure to air even for a few minutes oxidizes the fissures in the Pb sufficiently that even atomic hydrogen cannot pass.

Finally we turn our attention to Fig. 7 which shows a hydrogen-implanted junction for both bias polarities. In curve *a* the electron travels from the Al- to the Pb-enhancing structure nearest the lead,[30,31] while in curve *b* it is more sensitive to the structure at the Al-oxide interface. These curves suggest that the 230 and 115 meV structures are associated with modes nearer the Al, while the O—D bend near 80 meV and the stretch near 450 meV arise due to groups closer to the Pb.

IV. SUMMARY

The most important conclusion to be reached is that the structure near 230 meV is not a harmonic of the Al—O stretching peak near 115 meV as had been commonly be-

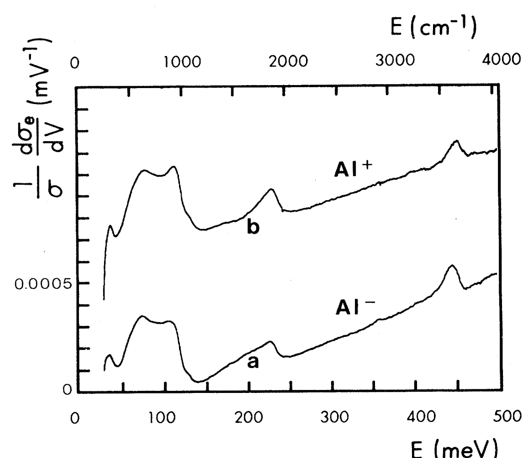

FIG. 7. Spectrum of a typical hydrogen-implanted junction with the Al biased positively.

lieved. We have clearly demonstrated that this 230-meV peak is due to hydrogen and the absence of any strong O-H bands in the infrared or Raman spectra aluminum oxides or hydroxides suggest that this peak may be due to aluminum hydride. We have also demonstrated that Al-oxide—Pb junctions can be prepared with very small amounts of surface O—H stretch (near absence of the 450-meV stretch) with the use of a Meissner trap during preparation. In the case of hydrogen-implanted junctions we have shown that hydrogen is very mobile in these junctions. Implantation can lead to large amounts of hydrogen in the virgin junction which will revert in time to an equilibrium concentration. This process can be accelerated by applying an external field. The nature of these oxides is important when using Al-oxide—Pb in studies where the oxide forms the active adsorbing layer. Finally oxides prepared using an ion gun contain far more hydrogen than those prepared by conventional plasma techniques and hence are of no advantage in IETS studies.

ACKNOWLEDGMENTS

We wish to thank R. V. Coleman, P. K. Hansma, A. M. Johnson, M. K. Konkin, and T. A. Will for many useful discussions. D. P. Mullin provided valuable technical assistance throughout this work. This work was supported in part by Natural Sciences and Engineering Research Council, Canada.

---

*On leave from the Institute of Physics, Polish Academy of Sciences, Warszawa, Poland.

[1] *Tunneling Spectroscopy: Capabilities, Applications, and New Techniques,* edited by P. K. Hansma (Plenum, New York, 1982).
[2] J. Lambe and R. C. Jaklevic, Phys. Rev. 165, 821 (1968).
[3] A. L. Geiger, B. S. Chandrasekhar, and J. G. Adler, Phys. Rev. 188, 1130 (1969).
[4] R. Magno and J. G. Adler, Phys. Rev. B 13, 2262 (1976).
[5] W. M. Bowser and W. H. Weinberg, Surf. Sci. 64, 377 (1977).
[6] D. G. Walmsley and W. J. Nelson, *Tunneling Spectroscopy: Capabilities, Applications, and New Techniques,* Ref. 1, Chap. 11.
[7] R. A. Dragoset, E. S. Phillips, and R. V. Coleman, Phys. Rev. B 26, 5333 (1982).
[8] R. C. Jaklevic and M. R. Gaerttner, Appl. Phys. Lett. 30, 646 (1977).
[9] R. C. Jaklevic and M. R. Gaerttner, Appl. Surf. Sci. 1, 479 (1978).
[10] J. L. Heiras and J. G. Adler, Appl. Surf. Sci. 10, 42 (1982).
[11] M. K. Konkin and J. G. Adler, J. Appl. Phys. 50, 8125 (1979).
[12] M. K. Konkin and J. G. Adler, J. Appl. Phys. 51, 5460 (1980).
[13] M. K. Konkin and J. G. Adler, J. Appl. Phys. 53, 5057 (1982).
[14] A. M. McIlraith, J. Vac. Sci. Technol. 9, 209 (1972).
[15] J. Franks and A. M. Ghander, Vacuum 24, 489 (1974).
[16] J. Franks, J. Vac. Sci. Technol. 16, 181 (1979).
[17] J. G. Adler and J. Straus, Rev. Sci. Instrum. 46, 158 (1975).
[18] J. G. Adler, in *Tunneling Spectroscopy: Capabilities, Applications, and New Techniques,* Ref. 1, Chap. 14.
[19] W. F. Brinkman, R. C. Dynes, and J. M. Rowell, J. Appl. Phys. 41, 1915 (1970).
[20] M. K. Konkin, R. Magno, and J. G. Adler, Solid State Commun. 26, 949 (1978).
[21] E. E. Huber, Jr. and C. T. Kirk, Jr., Surf. Sci. 5, 447 (1966).
[22] J. L. Erskine and R. L. Strong, Phys. Rev. B 25, 5547 (1982).
[23] P. Hofmann, W. Wyrobisch, and A. M. Bradshaw, Surf. Sci. 80, 344 (1979).
[24] T. Fort, Jr. and R. L. Wells, Surf. Sci. 32, 543 (1972).
[25] G. A. Dorsey, Jr., J. Electrochem. Soc. 113, 169 (1966).
[26] W. Vedder and D. A. Vernilyea, Trans. Faraday Soc. 65, 561 (1969).
[27] A. J. Maeland, R. Rittenhouse, W. Lahai, and P. V. Romanov, Thin Solid Films 21, 73 (1974).
[28] E. R. Lippincott, J. Chem. Phys. 17, 1351 (1949).
[29] L. A. Woodward and H. L. Roberts, Trans. Faraday Soc. 52, 1458 (1956).
[30] I. K. Yanson *et al.,* Zh. Eksp. Teor. Fiz. Pis'ma Red 62, 1023 (1972) [Sov. Phys.—JETP 35, 540 (1972)].
[31] John Kirtley, D. J. Scalapino, and P. K. Hansma, Phys Rev B 22, 3177 (1976).